ELSEVIER

Biophysical Chemistry 58 (1996) 53–65

Biophysical Chemistry

Temperature dependent intermediate structures during the main phase transition of dimyristoyl phosphatidylcholine vesicles a combined iodine laser–temperature jump and time resolved cryo-electron microscopy study

Rainer Groll, Artur Böttcher, Joachim Jäger, Josef F. Holzwarth *

Fritz-Haber-Institut der Max-Planck-Gesellschaft, D-14195 Berlin-Dahlem, Germany

Received 24 January 1995; revised 11 May 1995; accepted 15 May 1995

Abstract

The kinetics of the main phase transition of dimyristoylphosphatidyl choline (DMPC) unilamellar vesicles were investigated in the time range from microseconds to seconds. Iodine laser–temperature jump (ILTJ) experiments showed three discrete relaxation phenomena. Time resolved cryo-electron microscopy (CEM) was applied to produce images of intermediate states typical for the relaxation times of lipid vesicles in the micro- to millisecond time window. A careful measurement of the rate of temperature decrease observed during the production of vitrified lamellae of aqueous samples on a copper grid was performed. The best conditions resulted in average rates of cooling of 3×10^4 K/s. By comparing the images from CEM of DMPC vesicle samples vitrified above, at, and below the phase transition temperature a structural model was designed, which explains the temperature jump relaxation times in the micro- to millisecond time range by the formation and disappearance of coexisting clusters of crystalline, intermediate, and fluid lipid areas inside the DMPC bilayers.

Keywords: Dimyristoyl phosphatidylcholine vesicles; Lipid-phase transition; Laser temperature jump; Cryo-electron microscopy; Vitrified aqueous lamella

1. Introduction

The main phase transition of lipid mono- and bilayers from the crystalline to the fluid state has been an area of intensive research. The reason for such investigations is not only to clarify the underlying physical questions of the type of transition, but also to contribute to the more complex behavior of biological membranes and cells. In recent years the established idea of a pure first order phase transition has been questioned. New results especially on monolayers [1,2] suggested that this transition from a crystalline to a fluid phase is not simply of first order but stems from superimposed orders of transition, i.e., a first order transition to which higher order transitions are superimposed [2]. We have investigated the dynamics of pure and functional proteins containing lipid vesicles extensively using our ILTJ technique. Five well time-separated relaxation sig-

* Corresponding author.

SSDI 0301-4622(95)00085-2

nals between 4 ns and 100 ms [3–5] were characterized. The molecular interpretation of these relaxation phenomena is becoming increasingly demanding and more complex the longer the relaxation time. The principle problem of deducing mechanisms and molecular models from relaxation measurements is added to the dilemma. To overcome our problems we started to combine ILTJ experiments with structural methods of high space resolution like electron microscopy. The main difficulty was to stabilize temperature dependent intermediate structures of lipid vesicles which might be typical for certain relaxation phenomena in the micro- to millisecond time range in such a way that they can be inspected in an electron microscope (EM). EM is a slow technique and at least minutes are needed to achieve an image.

Stabilizing our samples by fast freezing which was pioneered by Taylor and Glaser [6], Unwin and Henderson [7] and first applied to lipid systems by Dubochet and coworkers [8] seemed to be a promising way. Heide and Zeitler [9] had established the method of forming amorphous ice at the temperature of liquid nitrogen at the Fritz-Haber-Institut. The main question was, if it was possible to stabilize structures of lipid vesicles typical for short living intermediates during the phase transition without the need of any staining material or the production of a replica of the surface structure as is done in freeze fracture experiments. Vitrification of the intermediate structures of interest in amorphous ice to inspect and characterize them in a CEM looked like the best way to achieve our goal and minimize at the same time artifacts caused by the stabilizing procedure.

The combination of dynamic information from IL–temperature jump experiments and real structural information from CEM should allow us to construct a more refined picture of the relaxation processes of DMPC vesicles undergoing a phase transition around room temperature in the micro- to millisecond time range.

2. Materials and methods

2.1. Chemicals

Dimyristoyl phosphatidylcholine was purchased from Fluka (Switzerland). The buffer solutions (pH 7.5) consisted of 0.01 M tris(hydroxymethyl)aminomethane (Fluka), 0.1 M NaCl (Merck, Germany) and 1 mM NaN_3 (Merck) in triply distilled water. All chemicals were of the highest purity available and were used without further purification.

2.2. Vesicle preparation

The vesicles of DMPC were prepared by a 'modified injection method' [10]. 30 μM of DMPC were dissolved in 1 ml ethanol and slowly injected (30 min) with a Hamilton syringe into 10 ml of pure buffer at 30°C and then dialyzed above the phase transition temperature (T_{MPT}) of 23.5°C against pure buffer for at least 8 h. Vesicles were characterized by turbidity–temperature phase transition curves and differential scanning calorimetry (DSC, MicroCal, Northampton, USA) and electron microscopy. Special care was taken that the equilibrium turbidity of the preparations did not change during the experiments.

Fig. 1a shows the result from a DSC experiment and Fig. 1b a typical turbidity–temperature measurement performed in a Perkin Elmer spectrophotometer. The temperature scan rate in Fig. 1b was 0.2°C/min. The solid line is the continuous upscan result and the circles are equilibrium measurements after a full scan to demonstrate the reproducibility and stability of the samples.

2.3. Iodine laser–temperature jump (ILTJ)

Our ILTJ instrument was used in the oscillator mode with a time resolution of 2.4 μs producing T-jumps of approximately 1 K in 150 μl heated volume. Details of the experimental setup are reported in the literature [8,11,12]. A schematic diagram is given in Fig. 2 and Table 1 summarizes the details of the ILTJ and a comparison with commercial Joule heating instruments.

ILTJ is especially useful for highly aggregated biological systems because the T-jump is achieved by photon absorption of rotational vibrational states of the solvent water at 1.315 μm. High transient electric fields (15–40 kV/cm) typical for Joule heating instruments are completely avoided. There are no restrictions on the detection parameter besides that it

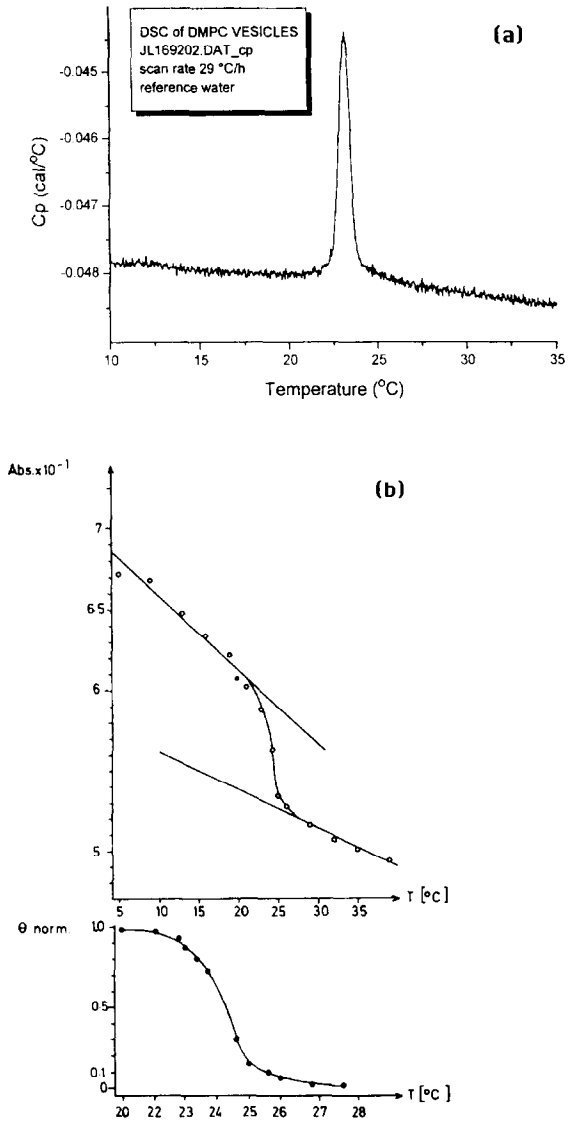

Fig. 1. (a) Temperature energy transfer measurements for DMPC vesicles in pH 7.5 buffer performed in a differential scanning calorimeter (DSC) using an upscan rate of 29°C/h. The maximum appears at the midpoint of the main phase transition. (b) Equilibrium turbidity–temperature phase transition curve of DMPC (= DML – DM-lecithin in the figure) vesicles of the radius R (60 nm) observes at 300 nm, 0.5 cm. The solid line is a continuous upscan of 0.2°C/min. The circles are test measurements at fixed temperatures and θ is the normalized order parameter temperature dependence from 20–28°C. Turbudity is shown at T around the maine phase transition

has to change with temperature (reaction enthalpy) and very small sample volumes (100 μl) can be used [13].

2.4. Cryo-electron microscopy

Experiments with a CEM can be divided into three steps:

1. Incorporation of the vesicles into amorphous ice.
2. Transfer of the vitrified sample into the CEM at ca. 70 K.
3. Inspection of the frozen sample in the CEM at or below 70 K.

The instrument we used was a home made CEM (DEEKO 250) in the transmission mode, allowing for a space resolution for vitrified lipid samples of 1–2 nm.

We shall focus here on the first step of the experiment, the incorporation of lipid vesicles into amorphous ice. The time needed for stabilizing the samples at low temperatures (at least below 150 K) dominates the time range in which we can hope to gain structural details from intermediate states typical for the micro- to millisecond time window. Fig. 3 contains a schematic diagram of a vitrified lamella of the sample and how the image is achieved by scattering of electrons at the location of the embedded vesicles. The amorphous ice does not cause any typical scattering besides homogeneously weakening the electron flux at the position of the image plate. Only the part of the lamella with a thickness below 500 nm can be used because of intensity problems with thicker lamellae. It is a prerequisite for any further investigation to prove that the ice of the lamellae on the grid is amorphous and stays in that state during the experiment. Ice crystals could enforce a structure on the vesicle bilayer and would therefore not allow the imaging of the true structural details! Fig. 4 shows the scattering patterns from the electron transmission mode of three states of ice formed inside lamellae of vitrified water:

1. Amorphous ice – no special patterns;
2. Small ice crystals – some shadowing around the center;
3. Large ice crystals – clear scattering structures.

The inspection of the vitrified lamellae before further experiments are performed is inevitable and was always done to ensure amorphous ice. Fig. 5 shows the arrangement for measuring the time needed to form the lamellae of vitrified samples on a copper grid (see also Fig. 3). A thermocouple of 0.2 mm size was fixed on the grid normally and is used to

hold the samples. The grid could be shot by a spring mechanism into the cooling liquid. Very thin electric wires are connected to an oscilloscope and a transient recorder to register the voltage changes due to the temperature changes of the grid by entering the cooling liquid. The whole arrangement had a time

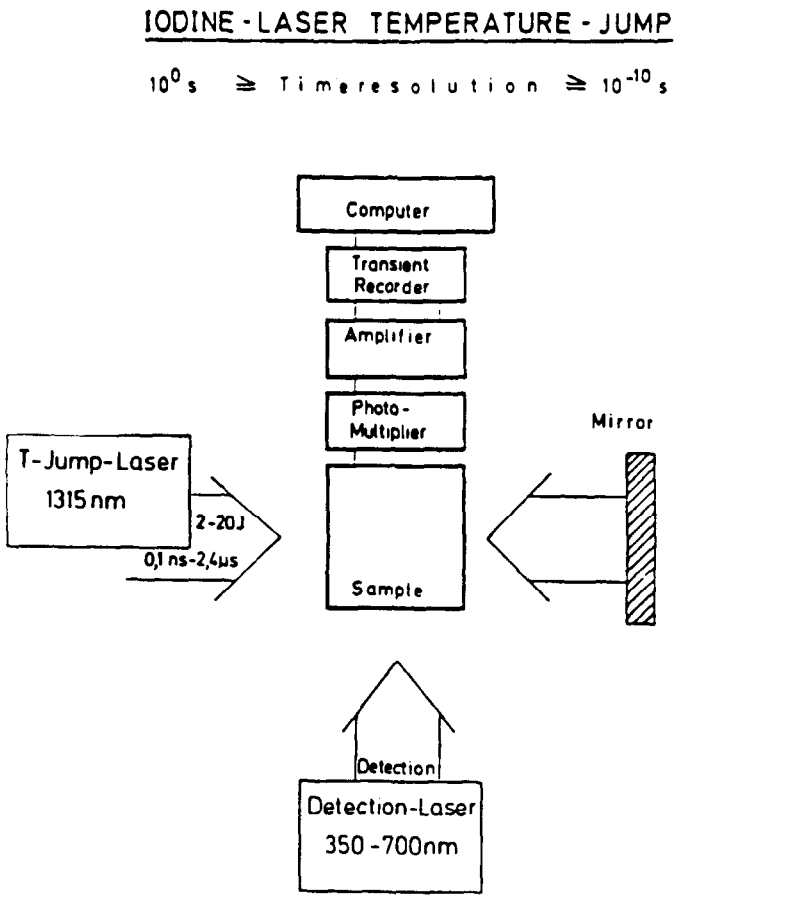

Fig. 2. Principle experimental arrangement of the iodine laser–temperature jump (ILTJ), including a summary of the advantages and characteristics.

resolution better than 100 ns. In Fig. 6 the response of the thermocouple to temperature changes is reported for later conversion of voltage changes into temperature changes. The signals could be further processed in a computer system. The same arrangement as in Fig. 5 (without the thermocouple, wires and detection system) was used to form the vitrified DMPC vesicle samples for inspection in the CEM.

Fig. 7 reports the cooling rate of the grid in dependence of the type of coolant. It is clearly seen that liquid nitrogen itself is not a good coolant because of the formation of nitrogen gas layers which act as an insulator after entry of the grid into liquid nitrogen. Liquid propane at 70 K is much better for fast cooling because it does not form an insulating gas layer during the cooling process on the surface of the grid. Fig. 8 demonstrates the influence of the entry velocity of the grid into liquid propane.

Table 1
Summary of physical characteristics and already performed applications of the iodine laser temperature jump (ILTJ) technique

IODINE LASER TEMPERATURE JUMP (ILTJ) for WATER (or -OH) containing SOLUTIONS
Timeresolution 10^{-9}s to 10^{0}s

Josef F. HOLZWARTH et al.

(I)	**Direct absorption of T-jump energy by solvent OH-groups:**	**Independent of solution composition**
(II)	**Water absorption by overtone vibrations:**	**Suitable wavelength (1.31 μm)** **Extinction coefficient (0.76/cm)**
(III)	**I L T J limits:**	**Emission time of IL ($> 10^{-10}$ s)** **Power threshold H_2O ($1.5 .10^{10}$ W/cm^2)** **Back cooling time (10^{0} s)**
(IV)	**Detection system:**	**Fluorescence, Absorption,** **Light scattering, Conductivity,** **Circular dichroism, order parameter;** **Data sampling and processing**
(V)	*Joule-Heating for comparison:*	*High electrolyte conc. needed (0.1 M)* *Disturbing trans. elec. field (~30 kV/cm)* *Time resolution ($> 10^{-6}$ s)*

APPLICATIONS of I L T J

(1) Proton transfer
(2) Electron transfer
(3) Conformation and Aggregation changes
(4) Dynamics of Micelles and Microemulsions
(5) Kinetics of Lipid - Bilayer systems, Membranes
(6) Enzyme reactions
(7) DNA - Dye interactions
(8) Polymer Dynamics in solution
(9) General Solution Dynamics from 10^{-9} to 10^{0} seconds

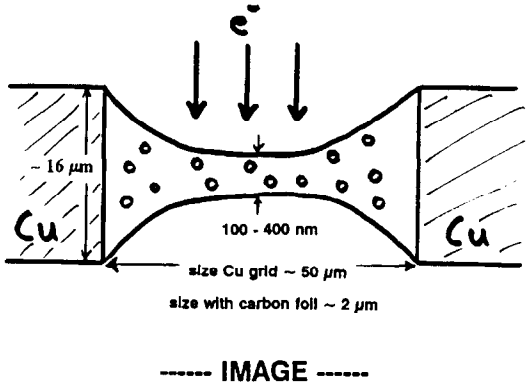

Fig. 3. Schematic drawing of a vitrified lamella containing vesicles and some important sizes of the copper grid used. The central part of the lamella has the correct thickness for images.

Entry velocities above 6 m/s are dangerous as they might destroy the lamellae by cavitation effects occurring during the entering of the grid into liquid propane and before vitrification is complete. We typically used approximately 4–5 m/s as entry velocity. Fig. 9 contains a very important result as it shows that the amount of water on the grid is extremely influential for the time needed to stabilize short living intermediate structures of embedded vesicles, i.e., rate of temperature decrease. An explanation for this behavior is simply given by the amount of heat transfer needed to reach the desired low temperature. We can learn from Fig. 9 that small amounts of water, thin lamellae, are preferred for fast temperature changes resulting in high time resolution. We also deduce that the best stabilizing time for intermediate structures which can be achieved should be longer than 100 μs because at least 150 K has to be reached to immobilize structural changes. This value is dependent on the type of system chosen for investigation and can not be taken as a general constant.

3. Results and discussion

The dynamics of the main phase transition (MPT) of DMPC and DPPC unilamellar vesicles of 20–70 nm size was characterized by ILTJ experiments in our group before [3–5,13,14]. Different detection techniques like time resolved equilibrium fluorescence anisotropy lifetimes [4], turbidity and light absorption [13] were used. The influence of membrane polypeptides or proteins [13] and cholesterol [14] on MPT were studied. Here we concentrate on unilamellar vesicles of DMPC of 30–100 nm size and shall investigate the time range from 1 μs to 1 s to learn about the possibility of achieving CEM images from intermediate structures typical for the dynamic phenomena associated with MPT. There are two reasons for this: first the cooling rate of lamellae containing vesicles is not fast enough to stabilize intermediate structures with lifetimes shorter than 50 μs, second the thermodynamic inspection of the five

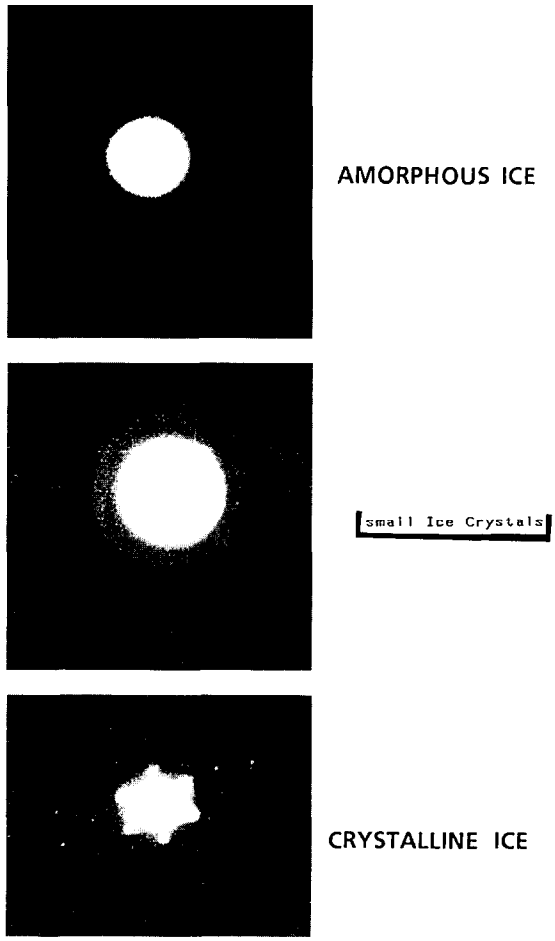

Fig. 4. Electron diffraction patterns of – amorphous ice, small ice crystals, and fully crystallized ice – measured by transmission electron microscopy of lamellae of vitrified samples on a copper grid as in Fig. 3.

relaxation processes we measured as characteristic for MPT between 1 ns and 1 s lead us to the conclusion that 80% of the enthalpy change (ΔH) is associated with the relaxation phenomena in the micro- to millisecond time regime [13]. Those results were achieved by careful inspection of the relaxation amplitudes of the five relaxation signals measured under similar conditions and after a 2 ns T-jump. (The relaxation amplitudes are dependent on the ΔH of reaction through the Van't Hoff equation: $\mathrm{d}\ln K/\mathrm{d}T = \Delta H \Delta T/RT^2$). Fig. 10 summarizes the relaxation times and their corresponding relaxation amplitudes after a 2.4 μs T-jump of 1 K.

Unilamellar vesicles of DMPC of 2.7 mM concentration prepared at pH 7.5 were used and turbidity was the detection parameter. The temperatures indicated are always initial temperatures before the T-jump, because this temperature can be controlled inside 0.1 K. The uncertainty of the T-jump is sometimes 0.2 K. It is clearly seen that relaxation times and their corresponding amplitudes show pronounced maxima at the midpoint of MPT indicated

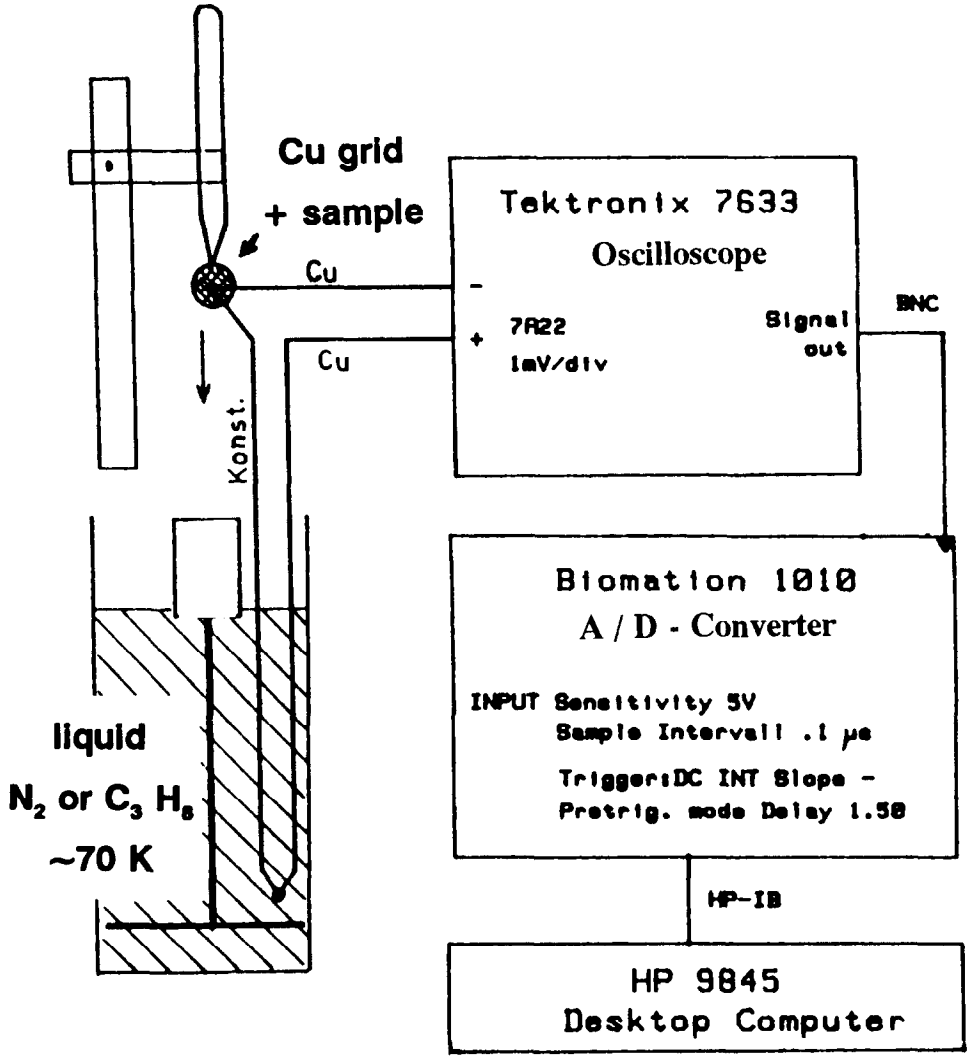

Fig. 5. Experimental arrangement for fast cooling, showing the copper grid which holds the sample solution. The spring mechanism for shooting the grid into the cooling liquid and the wires as well as the detection arrangement for measuring the cooling rate are seen.

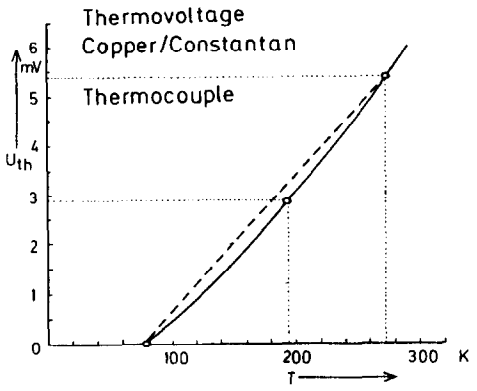

Fig. 6. Voltage–temperature response of the copper/constantan thermocouple (0.2 mm in size) applied in the measurements of the cooling rate.

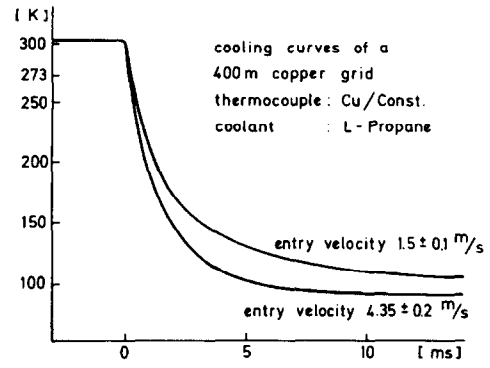

Fig. 8. Entry velocity dependence of the cooling rate of a copper grid by liquid propane.

on the figure as T_{MPT}. Such a behavior results from the increasing co-operativity of the relaxation processes approaching T_{MPT}. We have learnt from other experiments that the maximum at T_{MPT} increases with decreasing values for the T-jumps ΔT. Signal to noise problems did not permit ΔT values much smaller than 1 K. The time maxima of the three relaxation processes shown in Fig. 10 at T_{MPT} are caused by a 'critical slowing down' of the dynamic phenomena responsible for the phase transition [15]. From time resolved measurements of turbidity [13], quasi equilibrium fluorescence anisotropy [4,5], and absorption of lipid probe molecules like acridine-orange lipids [13] we developed a dynamic model describing the phase transition by molecular changes (Fig. 13). The first relaxation around 4 ns was attributed to the formation of simple rotational isomers in the hydrocarbon chains [3] and the relaxation around 100 ns is strongly influenced by the type of headgroup of the lipids. In other words these changes are due to dynamic phenomena more typical for single molecules and therefore less cooperative than the relaxations especially investigated in this paper. The relaxation times observed after 1 μs are more complex in nature and a satisfactory molecular description is very hard because the interplay of molecular assemblies has to be taken into account. We know from the observation of diffusion of labelled lipids in the bilayer matrix of DMPC or DPPC that the process of lateral diffusion is already observable some microseconds after a nanosecond T-jump around T_{MPT}.

The cooling times measured in Fig. 9 lead us to

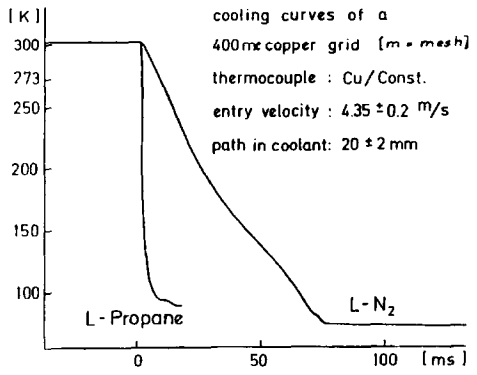

Fig. 7. Cooling rates of the copper grid for liquid propane and liquid nitrogen as coolants.

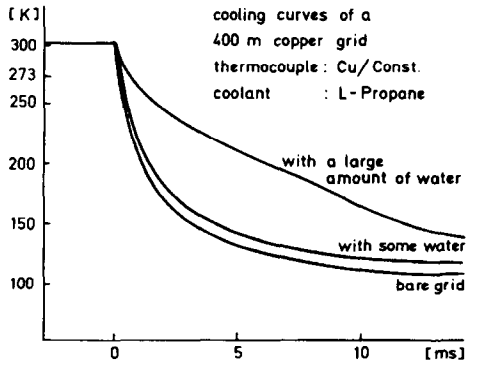

Fig. 9. Cooling rate dependence of water lamellae on a copper grid (see Fig. 3) with different amounts of water, i.e., different thickness of lamellae; coolant liquid propane.

the conclusion that it should be possible to stabilize intermediate structures of lipid assemblies typical for the relaxations after 50 μs. In Fig. 11a and b we show CEM images measured for unilamellar DMPC vesicles which were vitrified starting above and below the phase transition T_{MPT}. The pictures clearly demonstrate that the vesicles vitrified from a starting temperature well above T_{MPT} (Fig. 11a) are perfect circular spheres with almost no structural details. They do not allow a differentiation between the inner and the outer half of the bilayer. The contrast in the images from CEM is mainly due to the headgroups of the lipids in the bilayer. DMPC vesicles vitrified from temperatures well below the phase transition T_{MPT} are imaged in Fig. 11b. Here we see structural details to such an extent, that we can separate the outside from the inside of the lipid bilayer. Furthermore, we see a facetted surface which did not appear in Fig. 11a.

To clarify the question of the appearance of the facetted surface we vitrified unilamellar DMPC vesicles in the temperature range of the phase transition T_{MPT}. Fig. 12 summarizes these experiments. Vesicles vitrified from temperatures above T_{MPT} never showed facetted surfaces, if amorphous ice was present. Vesicles vitrified from temperatures next to T_{MPT} showed the onset of facetted surfaces. Vesicles vitrified from temperatures below T_{MPT} always showed strongly facetted surfaces and a difference in contrast of the images to allow for distinction between the inner and outer layer of lipids. Fig. 12 also shows our model explanation on a molecular scale. The idea behind this model picture is further exploited in Fig. 13. Here we have modeled the five relaxation phenomena of the lipid phase transition of DMPC vesicles measured in ILTJ experiments and indicated the time ranges for ILTJ measurements (10^{-9}–10^{0} s) as well as the time window in which vitrified vesicles can show images of intermediate structures typical for the phase transition of DMPC. If we combine our experiments to investigate the rate of structural changes characteristic for the main phase transition of unilamellar vesicles of DMPC, i.e., ILTJ investigations and CEM inspections of vitrified

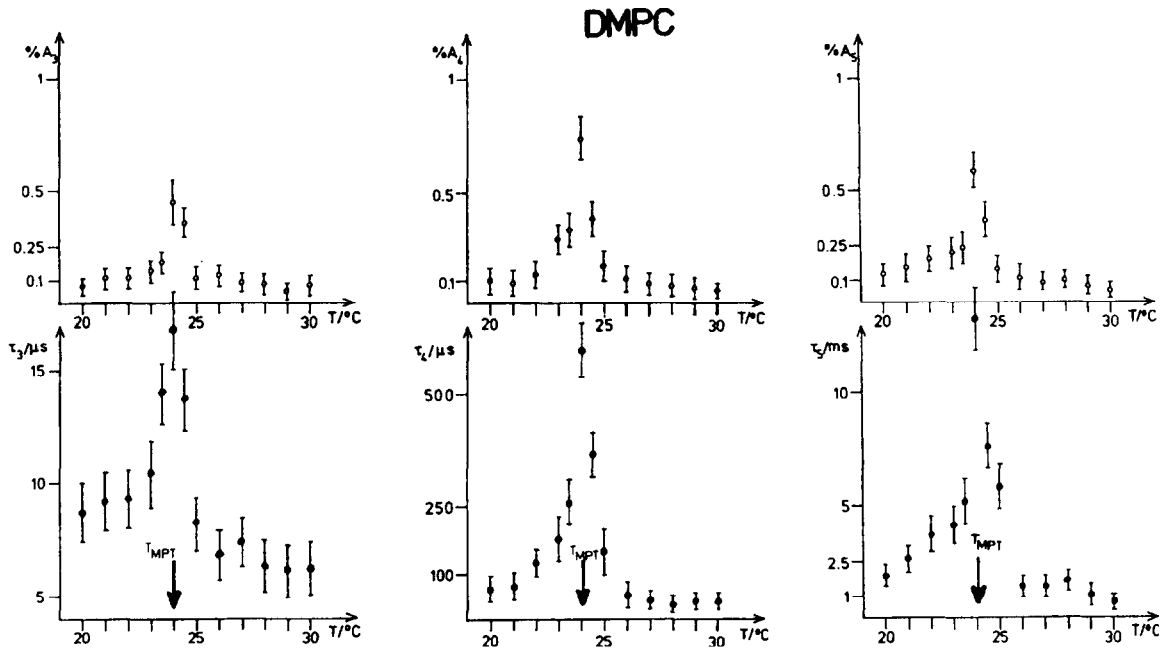

Fig. 10. Iodine laser temperature jump relaxation measurements of unilamellar DMPC vesicles of 2.7 mM concentration observed in the temperature range of the main phase transition from 20–30°C. Relaxation amplitudes A and the corresponding relaxation times τ are indicated for the starting temperatures of the T-jump experiments. T_{MPT} represents the main phase transition temperature from equilibrium measurements as in Fig. 1a and b.

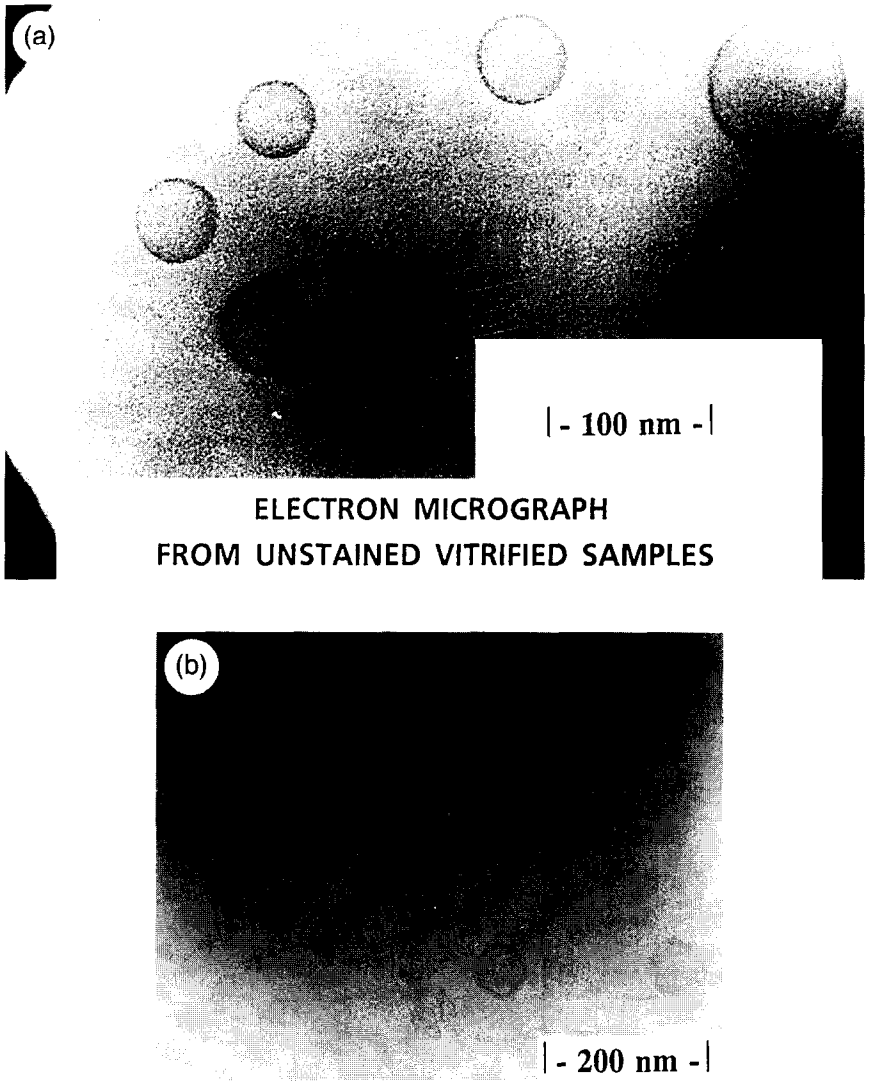

Fig. 11. (a) Electron micrograph of DMPC vesicles vitrified from a starting temperature above the phase transition. The perfect spherical structures of the vesicles are documented and no flat crystalline areas are monitored; the vesicles are in the fluid state. (b) Electron micrograph of DMPC vesicles vitrified from a starting temperature well below the phase transition. The facetted surface and details of the outer- and innerhalf of the bilayer can be distinguished. This is an equilibrium state, but the absolute location of the flat areas on the surface can change.

DMPC vesicles we can conclude that the MPT is not a simple first order transition in which only two states, the fluid and the crystalline state, are existing. Intermediate states of order seem to be possible and the existence of crystalline domains surrounded by intermediate states of order and further away by fluid lipid structures might dominate the micro- to millisecond time range. This interpretation is based on theoretical ideas first introduced by Adam [16] later used by Tsong and Kanehisa [17] for the interpretation of relaxation signals from lipids and more recently exploited by Mouritsen [18] in Monte Carlo simulations. Mouritsen incorporated up to 10 intermediate states of order in his calculations; unfortunately Monte Carlo simulations do not include an absolute time scale, but tell the sequence of events

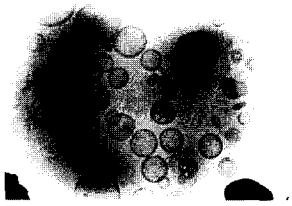

COOLING STARTED ABOVE
PHASE TRANSITION TEMPERATURE

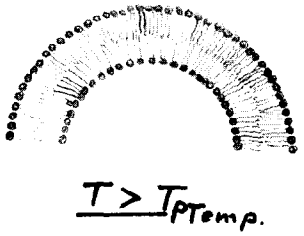

CURVED FLUID DOMAINS

COOLING STARTED AT
PHASE TRANSITION TEMPERATURE

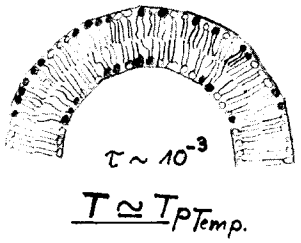

INTERMEDIATE STRUCTURES

COOLING STARTED BELOW
PHASE TRANSITION TEMPERATURE

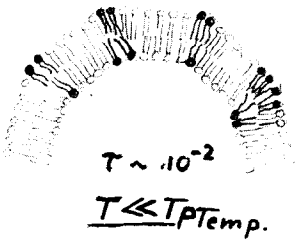

FLAT CRYSTALLINE DOMAINS

Fig. 12. Summary of electron micrographs and corresponding molecular models for vitrified unilamellar DMPC vesicles characteristic for starting temperatures of the cooling process above, at and below the phase transition temperature. Regularly curved fluid domains, intermediate structures with some flat crystalline areas and facetted structures containing mainly crystalline areas are clearly distinguishable.

on a relative time scale. His simulations showed domain formation and disappearance as the last events occurring.

We believe that our time resolved experiments, ILTJ and CEM, in the micro- to millisecond time window (signals 4 and 5 in Fig. 10) can be interpreted as follows: The two slowest signals from the phase transition are attributed to the coexistence of domains of different order stabilized by intermediate states, which separate the extreme cases of crystalline and fluid states. Mouritsen and Zuckermann [19] used a microscopic interaction model which included a variable number of lipid chain conformational states. According to their model fluid areas coexist with more rigid clusters consisting of a mixture of all-trans hydrocarbon chain isomers together with lipids of intermediate order of their hydrocarbon chains. We attribute our signals 4 in Fig. 10 to the growth of the fluid areas associated with a decrease in size of the more rigid clusters. Signal 5 of Fig. 10 we connect with the disappearance of whole clusters which should show the highest co-op-

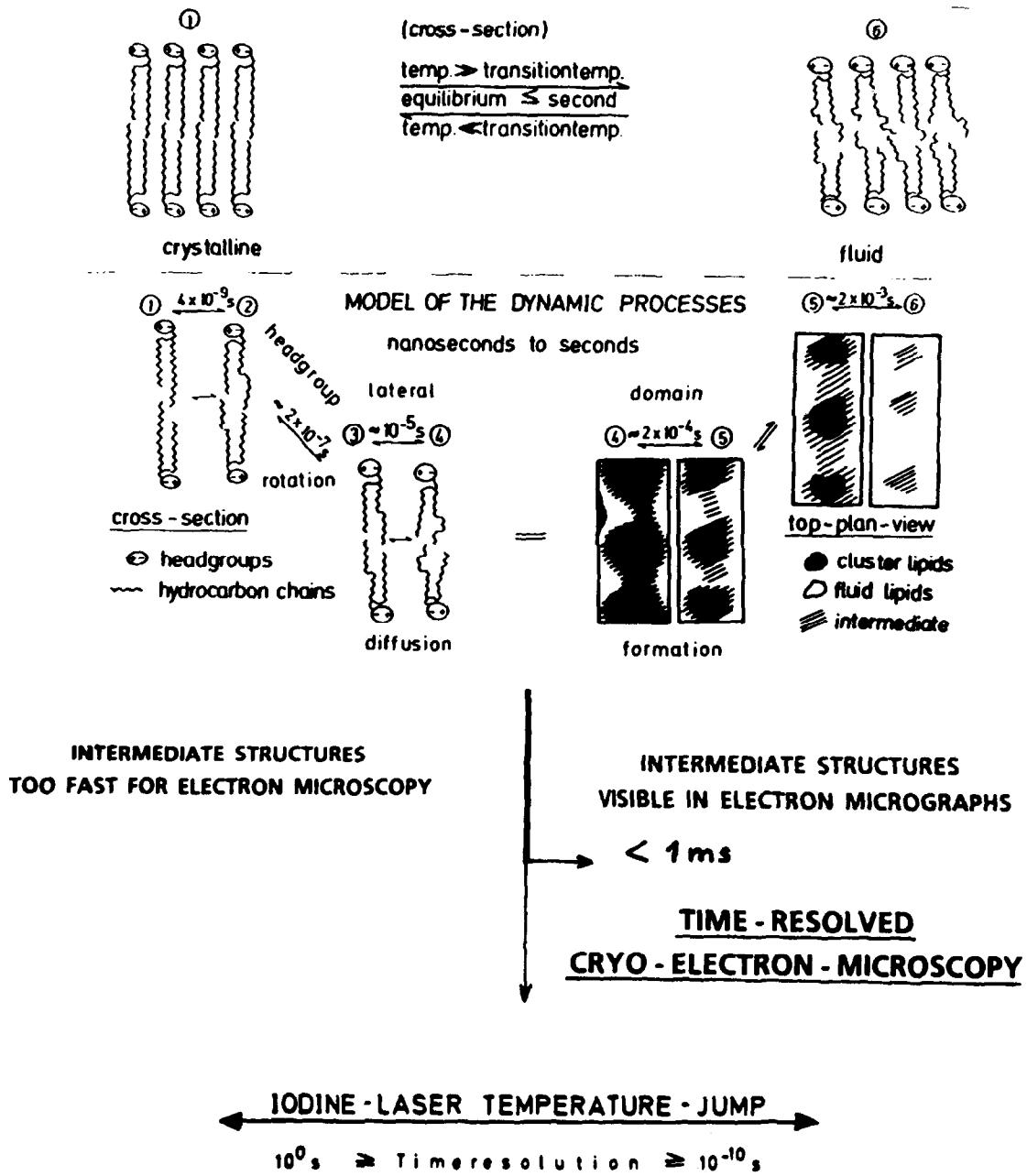

Fig. 13. Model of the main phase transition of unilamellar lipid vesicles deduced from iodine laser temperature jump experiments and time resolved CEM. ILTJ is capable for a time resolution of 10^{-9}–10^{0} s. CEM of fast vitrified vesicles can produce images of intermediate structures with life times longer than 0.5 ms.

erativity as seen in the experiments. The different CEM images in Fig. 11a and b back up our interpretation, because the more rigid clusters should enforce a planar structure of the bilayer and the fluid domains should allow for the strong curvature needed in areas where the facetted surface changes direction.

The idea of intermediate structures and strong curvature changes during the phase transition of lipid bilayers can explain the experimental observation of an unusually high and maximal rate of transversal diffusion of molecules through lipid bilayers around the main phase transition temperature.

4. Conclusion

In this paper we have demonstrated that CEM combined with fast freezing is a powerful tool to achieve images from short lived intermediate states of lipid bilayer structures without the need of any staining material and retaining the natural solution environment. The time limit for such images was clarified to be around 50 to 100 μs. The connection with our time resolved ILTJ experiments observed in the micro- to millisecond time range helped to further establish a useful time window for CEM and interpret kinetic relaxation results as structural changes of lipid domains of different order. Nevertheless, one should keep in mind that electron microscopy is a slow technique and structures with life times shorter than minutes can only be imaged by immobilizing structural changes in amorphous ice. The time needed to prepare the sample governs the time resolution of CEM.

Acknowledgements

J.F. Holzwarth thanks the Deutsche Forschungsgemeinschaft for continuous support during the development of the ILTJ technique.

References

[1] N. Denicourt, P. Tancrède and J. Tessié, Biophys. Chem., 49 (1994) 153.
[2] M. Flörsheimer and H. Möhwald, Colloids and Surfaces, 55 (1991) 173.
[3] B. Gruenewald, W. Frisch and J.F. Holzwarth, BBA, 641 (1981) 311.
[4] A. Genz and J.F. Holzwarth, Eur. Biophys. J., 13 (1986) 323.
[5] A. Genz and J.F. Holzwarth, Coll. & Polym. Sci., 263 (1985) 484.
[6] K.A. Taylor and R.M. Glaeser, J. Ultrastruct. Res., 55 (1976) 448.
[7] P.N.T. Unwin and R. Henderson, J. Mol. Biol., 94 (1975) 425.
[8] J. Dubochet, J. Lepault, R. Freeman, J.A. Berriman and J.-C. Homo, J. Microsc., 128 (1982) 219.
[9] H.G. Heide and E. Zeitler, Ultramicroscopy, 16 (1985) 151.
[10] J.M. Kremer, M.W. Esker, C. Pathmamanocharan and P.H. Wiersema, Biochemistry, 16 (1977) 3932.
[11] J.F. Holzwarth, A. Schmidt, H. Wolff and R. Volk, J. Phys. Chem., 81 (1977) 2300.
[12] J.F. Holzwarth, in W.J. Gettins and E. Wyn-Jones (Eds.), Techniques and Applications of Fast Reactions in Solution, D. Reidel, Dordrecht, 1979, p. 47–70.
[13] J.F. Holzwarth, in A. Cooper, J.L. Houben and L.C. Chien (Eds.), The Enzyme Catalysis Process, Plenum, London, 1989, p. 383–411.
[14] A. Genz, T.Y. Tsong and J.F. Holzwarth, Biophys. J., 50 (1986) 1043.
[15] J.F. Holzwarth and F. Rys, Progr. Coll. Polym. Sci., 69 (1984) 109.
[16] G. Adam, in H. Haken (Ed.), Synergistics: Cooperative Processes in Multicomponent Systems, B.G. Teubner, Stuttgart, 1978, p. 220–231.
[17] T.Y. Tsong and M.J. Kanehisa, Biochemistry, 16 (1977) 2624.
[18] O.G. Mouritsen, Biochim. Biophys. Acta, 731 (1983) 217.
[19] O.G. Mouritsen and M.J. Zuckermann, Eur. Biophys. J., 12 (1985) 75.